ELSEVIER

Biophysical Chemistry 55 (1995) 137–151

Biophysical Chemistry

Bacteriorhodopsin: the mechanism of 2D-array formation and the structure of retinal in the protein

Anthony Watts *

Department of Biochemistry, University of Oxford, South Parks Road, Oxford, OX1 3QU, UK

Abstract

Bacteriorhodopsin, the light driven proton pump of the extreme halophilic bacterium *H. salinarium*, is an integral membrane protein (M_r ca. 26000) which forms 2D arrays in the purple membrane of the bacterium. It is this feature which has permitted the use of electron diffraction methods to resolve the protein structure to some degree of atomic detail, although the prosthetic group has not been fully resolved. However, the features which induce the protein to form these arrays have not been previously clarified. We have now shown that the protein array formation is driven by specific interaction of the protein with the charged phospholipid, phosphatidyl glycerol phosphate (or the sulphate derivative), a major (ca. 60%) lipid of the bacterial host membrane. In addition, in an effort to provide further structural information about the chromophore, retinal, of this protein, the orientation of the individual methyl groups of retinal have been determined from solid state deuterium NMR studies of the deuterated chromophore when in the protein binding site. This approach to structural resolution of the prosthetic group is ab initio, agrees with other studies on the chromophore and resolves new features of the bound retinal to a high degree ($\pm 2°$) of precision. Here, these two studies on this integral membrane protein will be reviewed.

Keywords: Bacteriorhodopsin; Lipid–protein interaction; Solid state deuterium NMR; Electron microscopy; Biological membrane; Retinal chromophore

1. Introduction

Determining high resolution structural details of large integral proteins is still a major problem in membrane biology. Because of the many practical difficulties of working with detergent solutions of amphiphilic proteins which are generally available only in rather small amounts and are inherently unstable, and the difficulty of obtaining very pure material, there has been slow progress in crystallising and resolving the structure of integral membrane proteins by traditional crystallographic examination of 3D crystals. Indeed, only three such proteins are currently described in atomic details from X-ray crystallography [1].

An alternative way to resolve membrane protein structure is to use electron diffraction examination of 2D arrays of a protein in the membrane. In the ideal case there is sufficient long-range order in the structure to obtain diffraction from which molecular details can be obtained. However, very few proteins form 2D arrays spontaneously or in the natural envi-

* Corresponding author.

SSDI 0301-4622(94)00147-2

ronment. One such protein, bacteriorhodopsin, is found to form a 2D array in the natural purple membrane of the halophilic bacterium, *H. salinarium*. This feature of the protein, a proton pump which provides cellular energy from the proton gradient it creates upon photoreception, has permitted the structure to be resolved to 2.7 Å in the plane of the membrane and 10 Å across the membrane by electron diffraction methods [2]. Clearly, if the mechanism by which bacteriorhodopsin forms the 2D arrays can be understood, then other proteins may be induced into similar ordered arrays for electron diffraction studies. This phenomenon we have studied in a rigorous way using membrane protein reconstitution technology in which the composition and components of membranes can be precisely varied and manipulated [3]. Thus we have investigated the factors which permit the bacteriorhodopsin to form 2D arrays and, using freeze-fracture electron microscopy which is an ideal method for identifying protein arrays in membranes, produced even better resolved protein arrays than found in the purple membrane itself by this method [4].

Although structural features of bacteriorhodopsin have been well resolved to almost atomic detail for many parts of the protein backbone and associated residues, the chromophore itself is still not completely resolved. Only the bulk of the cyclohexene ring has been located by electron diffraction studies within the three dimensional structure of the protein. Neutron diffraction studies have enabled the positions of either end of the chromophore, both in-plane and in-depth within the protein to be determined [5]. Routine high resolution NMR methods, although highly successful in determining the structure of small to medium sized (M_r ca. 20000), non-aggregated globular proteins in isotropic solution, are not generally applicable to highly aggregated macromolecules with large relative molecular mass, such as an integral membrane protein in the lipid bilayer. Bacteriorhodopsin within the purple membrane, due to the very slow molecular rotation with respect to the applied field, is unable to give any high resolution NMR spectral features which can be used to deduce structural information. In addition to the problem of slow molecular motion, NMR spectra are highly anisotropic and thus have an angular dependence giving very broad spectral lines. However, this spectral envelope contains all the angular components of the nuclear interactions which we have exploited by studying deuterons placed at specific positions along the retinal chromophore. For this nucleus, the dominant quadrupolar interaction gives an angular dependence of the quadrupole splitting measured as the frequency separation between the two resonances. Based on an evaluation of this angular dependence of the deuterium spectral line-shape, it has been possible to determine the orientations of the individual C–CD_3 bond vectors with respect to the membrane normal. In this way, we have resolved the absolute alignment of the retinal chromophore whilst in the protein binding site and probed the subtleties of the protein environment on the retinal conformation [6–8].

2. Materials and methods

2.1. Purification and reconstitution of bacteriorhodopsin for electron microscopy

Bacteriorhodopsin has been traditionally purified from the purple membrane of *H. salinarium* [9] by solubilization using octyl glucoside or LDAO as detergents [10] but not as a lipid-free protein. By adaptation of methods devised by Huang et al. [11], it has been possible to isolate bacteriorhodopsin in detergent entirely free of endogenous phospholipids, namely diphytanyl phosphatidyl glycerol phosphate (PGP) and diphytanyl phosphatidyl glycerol (PG), these being the major (60% and 6%, respectively, of the total) lipid classes in the purple membrane (Fig. 1). This has been performed by isolating the purple membrane patches from harvested *H. salinarium* as described previously [10–12] and solubilizing the protein in Triton X-100. For detergent exchange, the solubilized protein was applied to a Sephadex G-75 column and eluted with 1% cholate and the protein fractions concentrated [12]. Phospholipids and protein were reconstituted from cholate by detergent dialysis over a period of 4–5 days and purified on a sucrose gradient to produce homogeneous protein–lipid complexes. The absorption spectrum for the reconstituted bacteriorhodopsin (λ_{max} at 560 nm) was similar to that of the native purple membrane fragments for all lipid environments tested.

Three types of reconstituted complexes have been produced at a range of lipid–protein mole ratios of up to 1200:1. In some complexes, the protein was reconstituted into only dimyristoyl (di-$C_{(14:0)}$) phosphatidylcholine bilayers [12], while in others bacteriorhodopsin was reconstituted with the polar lipid fraction from the purple membrane [4], or with dimyristoyl phosphatidylcholine and controlled amounts of the individual types of the purple membrane phospholipids added [3]. Finally, dimyristoyl phosphatidylcholine was inserted into purple membrane fragments from pure dimyristoyl phosphatidylcholine bilayers using a non-specific transfer protein (nsTP); the protein containing complexes were subsequently separated from unincorporated lipid vesicles by density gradient centrifugation [4].

Lipids were either from Sigma Chem Co. or isolated from the purple membranes as a polar lipid fraction or as individual components, using conventional isolation and purification methods with chloroform–methanol. Thin layer chromatography was employed to identify phospholipids against known standards in chloroform–methanol–ammonia solvents and using ammonium molybdate and charring for identification purposes. The phospholipid composition of complexes was also characterized by high resolution phosphorus NMR of the complexes solubilized in 4% sodium dodecyl sulphate [12].

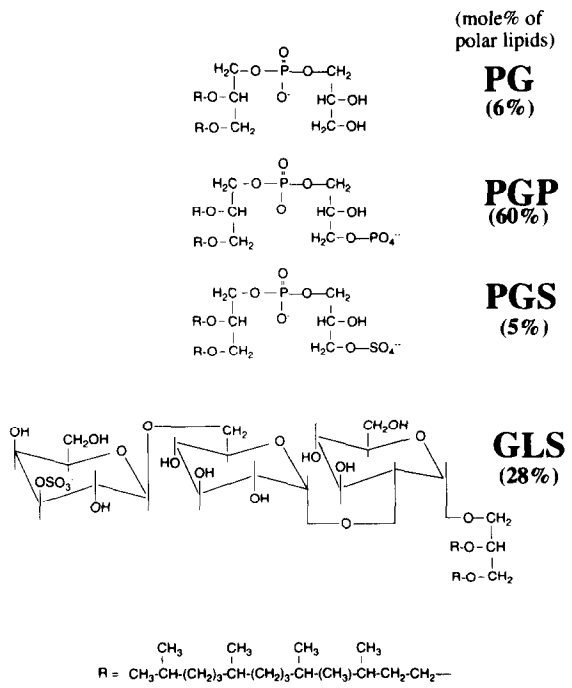

Fig. 1. Formulae of the major polar lipids of the purple membrane of *H. salinarium*. The lipids have almost exclusively diphytanyl alkyl chains (R). Phosphatidyl glycerol phosphate (PGP) comprises some 60% of the total membrane phospholipid whilst phosphatidyl glycerol (PG) and phosphatidyl glycerol sulphate (PGS) and sulphated glycolipids (GLS) form the remainder.

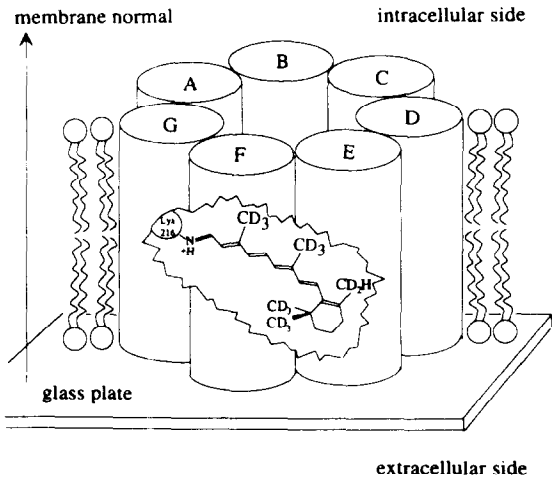

Fig. 2. Bacteriorhodopsin contains seven transmembrane α-helices in a single polypeptide chain. The chromophore, retinal, has been deuterated separately at each of the positions shown, in separate synthetic analogues with the given nomenclature of methyl groups C_{20}, C_{19} and C_{18} along the polyene chain from the point of retinal attachment site at the Schiff base (Lys-216) to the cyclohexene ring (methyls C_{16} and C_{17}), consecutively. The retinal was inserted into the protein in the chromophore binding site and uniaxially oriented purple membrane samples were prepared on small glass plates.

2.2. *Oriented purple membrane samples for NMR*

Various retinal derivatives, deuterated separately at the individual methyl groups in the polyene chain and cyclohexene ring (Fig. 2), were incorporated into bacteriorhodopsin by growing *H. salinarium* cells which were deficient in retinal synthesis (strain JW5). Purple membranes were isolated from lysed cells using standard procedures [9] and oriented on glass cover slips by controlled evaporation (85% humidity) over a period of 2 days in deuterium depleted

water to produce uniaxial films with good orientation of the purple membrane patches parallel to the sample plane [7]. A total of about 70–120 mg of bacteriorhodopsin (corresponding to 80 μmol of deuterons) was distributed over 15–18 plates that were mounted in a parallel stack inside a 10 mm NMR tube which could be placed in a horizontal coil for orientational studies. The membrane stack could be aligned with respect to the magnetic field with a precision of $\pm 3°$ and powder spectra were recorded from the samples after scraping off the membranes into a standard NMR tube.

2.3. Instrumental methods

Protein–lipid complexes as well as native *H. salinarium* cells were examined by freeze-fracture electron microscopy after quenching from a range of temperatures between 6 and 55° C. Samples were quenched at a rate of $> 10^4$ K/s using liquid propane and the sandwich method with plain faced sample holders; slower quenching rates of $< 10^4$ K/s were achieved with a cupped sample holder with a depression [12]. Samples were fractured and shadowed in a Balzars BAF-400D freeze-fracture machine. Cleaned replicas were examined in a Tesla BS-500 or Jeol-100B electron microscope. Optical and calculated diffractograms were made of selected arrays in the bilayer as a measure of the degree of protein order.

NMR measurements were carried out with a Nicolet 360 spectrometer operating at 145.9 MHz for phosphorus high resolution experiments of SDS solubilized complexes (relaxation delay of 2 s; MDP as reference). Wide-line deuterium NMR (at 61 MHz, quadrupolar echo with delay times around 30 μs, relaxation delays of 200 ms and a $\pi/2$ pulse width of around 5 μs) and phosphorus NMR (at 81 MHz, proton decoupling, pulse width of 4 μs, echo delays of 30 μs, relaxation delay of 1.3 s) spectra of oriented purple membrane fragments were recorded on Bruker MSL-400 and MSL-200 spectrometers, respectively [7].

2.4. Analysis of deuterium NMR spectra

Deuterium NMR spectral line-shapes are dominated by the orientationally-dependent quadrupolar interaction of the nuclear spin ($I = 1$) with the magnetic field, according to the nuclear spin Hamiltonian, $\mathscr{H}$[12]:

$$\mathscr{H} = \mathscr{H}_Z + \mathscr{H}_Q + \mathscr{H}_D + \mathscr{H}_{CS} \quad (1)$$

where the deuterium quadrupolar interaction $\mathscr{H}_Q \gg \mathscr{H}_D$ and $\mathscr{H}_{CS}$, the chemical shift and dipolar couplings respectively. In energetic terms, the static quadrupolar coupling constant (e^2qQ/h) is approximately 170 kHz for an aliphatic deuteron [13]. In the absence of motional averaging, the resonant line position ν_+ or ν_- for either of the $\Delta m_I = \pm 1$ transitions determines the quadrupole splitting, $\Delta\nu_Q$:

$$\Delta E/h = \Delta\nu_Q(\theta) = \nu_+ - \nu_-$$

$$= 3(e^2qQ/h)/4 \cdot (3\cos^2\theta - 1) \quad (2)$$

Thus, the angle (θ) of a deuterium bond vector with respect to the applied magnetic field can be calculated from the measured quadrupole splitting. When using labelled methyl groups, the quadrupolar interaction is reduced 3-fold due to the rapid spinning of the $-CD_3$ rotors, and the sensitivity of the signal is enhanced due to the narrowing of the spectral width, improved relaxation and the higher number of spins.

To determine the orientation of a deuteromethyl group on retinal in the protein prepared in a uniaxially aligned purple membrane sample, a conal distribution of bond vectors must be considered rather than the more usual spherical distribution for unoriented membrane dispersions. The resulting, complex line-shapes are rationalized by computer simulations of the deuterium NMR spectra, based on the probability density $p(\zeta)$ of a transition as a function of the reduced resonance frequency ζ, which describes the intensity envelope of the spectral line-shape [6,8]. For the static case of a conal distribution of $C–CD_3$ vectors assumed here, each calculated line shape contains up to three singularities (to be mirrored for $\Delta m_I = \pm 1$) which vary as a function of α and γ, the angles between the membrane normal and the applied field and between the bond vector and the membrane normal, respectively, as defined in Fig. 3. Angle ϕ is used only in the derivation of $p(\zeta_\pm)$, where it is taken through 0°–360° to cover the full range of deuterium vectors along the rim of the cone

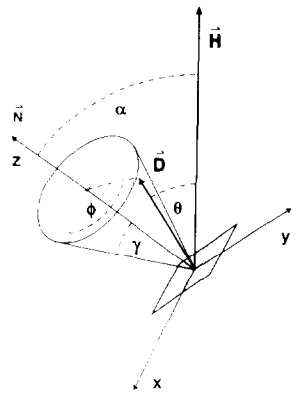

Fig. 3. For uniaxially oriented samples on a glass plate (shown as rectangle) at an inclination angle α with respect to the applied field, **H**, all immobilised but spinning $-CD_3$ groups lie along the rim of a cone with angle γ around the membrane normal, N. This axis coincides with the sample normal for the case of a perfectly oriented sample (with no mosaic spread). The spherical polar coordinates of **D** are γ (which is fixed) and ϕ. All vectors, **D**, contribute to the spectrum as ϕ is taken from 0° to 360°. The value of γ determines the quadrupole splitting, $\Delta\nu_Q$, at zero tilt, $\alpha = 0$, and the variation in ϕ in this conal distribution determines the complex line-shapes of the tilt series. From Ref. [6].

[6,7]. The total line shape is then given by the sum $p(\zeta) = p(\zeta_+) + p(\zeta_-)$, with:

$$p(\zeta)\left\{\sqrt{\frac{\pm 2\zeta_\pm + 1}{3}}\sqrt{\sqrt{\frac{\pm 2\zeta_\pm + 1}{3}} - \cos(\alpha + \gamma)}\right.$$
$$\left.\times\sqrt{\cos(|\alpha - \gamma|) - \sqrt{\frac{\pm 2\zeta_\pm + 1}{3}}}\right\}^{-1} \qquad (3)$$

Uniaxially oriented immobilized samples exhibit simple deuterium NMR spectra only when aligned with their normal parallel to the direction of the applied field ($\alpha = 0$) since then θ coincides with the cone angle γ and Eq. (3) reduces to the simple relationship given in Eq. (2). The spectrum is thus characterized by two lines with a quadrupole splitting $\Delta\nu_Q(\gamma)$ that is directly proportional to $(\cos^2\gamma)$:

$$\Delta\nu_Q(\gamma) = \Delta\nu_Q^{(\text{powder})} \cdot (3\cos^2\gamma - 1) \qquad (4)$$

where $\Delta\nu_Q^{(\text{powder})}$ is the value of a scaling factor (proportionally reduced from e^2qQ/h) that is measured from the powder line-shape of the sample. For all values of γ that lie between 35° and 90°, the sign of the quadrupole splitting is not known, only its magnitude. This complication can yield very different bond vectors for identical magnitudes but opposite signs of the quadrupole splitting. However, the sign can readily be resolved through recording a tilt series of spectra with the sample aligned at various angles, $\alpha \neq 0$, in the magnetic field [6,8] (but see below).

In practice, account must be made for the mosaic spread of the sample (mis-alignment) as well as for instrumental and other applied line-broadening factors [6,7]. Estimates of the sample mosaic spread

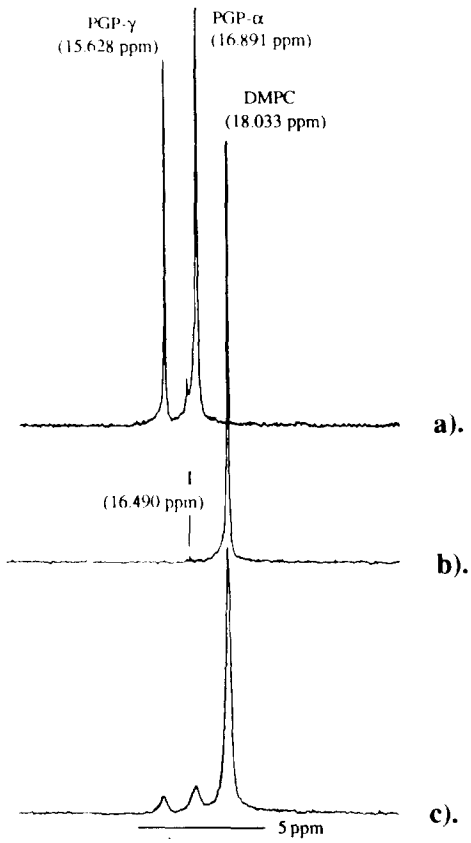

Fig. 4. High resolution phosphorus-31 (145.9 MHz) spectra of SDS solubilized complexes (4% SDS; 100 mM Tris–HCl, pH 7.4) containing bacteriorhodopsin from: (a) purified purple membranes; (b) a reconstituted bacteriorhodopsin–DMPC complex (1:68, protein:lipid mole ratio) with all the endogenous purple membrane phospholipids removed by detergent exchange; and (c) a reconstituted bacteriorhodopsin–DMPC complex (1:72, protein:lipid mole ratio) in which the protein was not delipidated. Chemical shifts are relative to MDP (not shown). From Ref. [11].

were made by recording the wide line phosphorus NMR spectra of the purple membrane phospholipids from the same samples as used for the deuterium NMR experiments, and simulating the line-broadening as a Gaussian contribution to the overall linewidth. This best-fitting value for the mosaic spread was then fixed into the deuterium spectral simulations to reduce the number of parameters required for these simulations. To account for instrumental line-broadening, a Lorentzian line-broadening contribution was also included in the spectral simulations in an equivalent way, based on the analysis of the unoriented powder line-shapes.

3. Results

3.1. Freeze-fracture electron microscopy of bacteriorhodopsin–lipid complexes

3.1.1. Bacteriorhodopsin–dimyristoyl phosphatidylcholine complexes

Phosphatidyl choline is a bilayer forming phospholipid which produces a zwitterionic (no net charge) bilayer surface to the polar medium. Thus, this lipid is ideally suited to the investigation of charge interactions between proteins and lipids, using reconsitution methods and controlled amounts of zwitterionic and charged lipids, such as phosphatidyl glycerol phosphate (PGP) (3 negative charges).

To confirm that the bacteriorhodopsin–dimyristoyl phosphatidyl choline complexes produced contain only dimyristoyl phosphatidylcholine and no residual PGP (Fig. 1) from the purple membrane, a reconstituted bacteriorhodopsin–dimyristoyl phosphatidylcholine complex, with low protein content to maximise the possibility of identifying any purple membrane phospholipids, has been solubilized in SDS and analysed by high resolution phosphorus NMR (Fig. 4) [12]. Here, no phosphatidyl glycerol phosphate signal was detected (< 2 PGP:1000 bacteriorhodopsin, mole:mole) confirming the complete delipidation of the protein before reconstitution, although samples produced with protein which had not been delipidated by column chromatography, did show some remaining (about 2 PGP:bacteriorhodopsin, mole:mole) phosphatidyl glycerol phosphate (Fig. 4).

Freeze-fracture electron micrographs of bacteriorhodopsin–dimyristoyl phosphatidylcholine complexes quenched slowly ($< 10^4$ K/s) show dispersed protein areas and protein-free lipid areas (Fig. 5a), the size of these areas depending upon the lipid:protein ratio [12]. In no case, over a very wide range of lipid:protein ratios, was any regular array formation of protein observed in such complexes. It therefore appears that protein–protein contacts or interactions alone are not sufficient for the bacteriorhodopsin to arrange itself into 2D-arrays in these zwitterionic lipid bilayers. Quenching the complexes

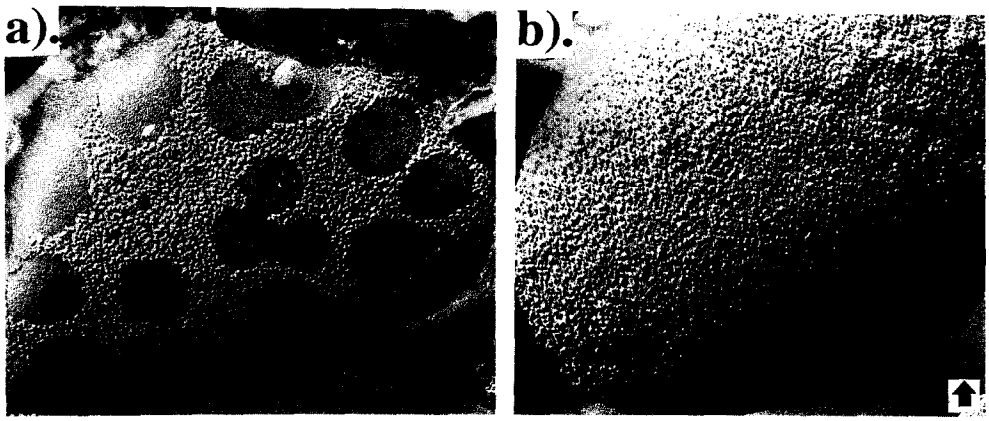

Fig. 5. Freeze-fracture electron micrographs of delipidated bacteriorhodopsin in reconstituted complexes with dimyristoyl phosphatidyl choline quenched at a (a) slow ($< 10^4$ K/s) and (b) fast ($> 10^4$ K/s) cooling rate from 45–55° C. Protein:lipid mole ratios are 1:180. Bar = 100 nm. Shadowing direction shown by arrow. From Ref. [11].

Fig. 6. Freeze-fracture electron micrograph of delipidated bacteriorhodopsin in complexes reconstituted with the polar lipid fraction from *H. salinarium*. Protein:lipid mole ratio is 1:7. Bar = 100 nm. Shadowing direction shown by arrow. The protein trimers are arranged in an hexagonal array as shown by the calculated diffractogram (upper inset) of a selected part of the complex and the correlation average of the diffractogram displayed as a relief contour map (lower inset). From Ref. [4].

slowly from a range of temperatures or salt and buffer conditions, has no effect on the appearance of the complexes.

Fast quenching ($> 10^4$ K/s) of the samples did not produce the patches of protein-free bilayer (Fig. 5b) implying that during fast quenching the protein did not have time to self-associate into laterally phase separated areas [12]. Even in very dense regions of protein, no hexagonal packing of the protein was again observed for a range of complexes under various conditions.

3.1.2. Complexes containing bacteriorhodopsin and polar lipids from the purple membrane

Bacteriorhodopsin reconstituted with the polar lipid fraction that was isolated and purified from purple membrane, gave rise to bilayer complexes in > 2 M NaCl (Fig. 6) [4]. In all complexes, a well defined hexagonal arrangement of the protein was observed, as shown in the optical diffractograms of selected areas of the bilayer. The Fourier transform of the calculated diffractograms to reconstruct relief profiles for the protein in the bilayer confirmed the hexagonal packing arrangement of the protein (Fig.

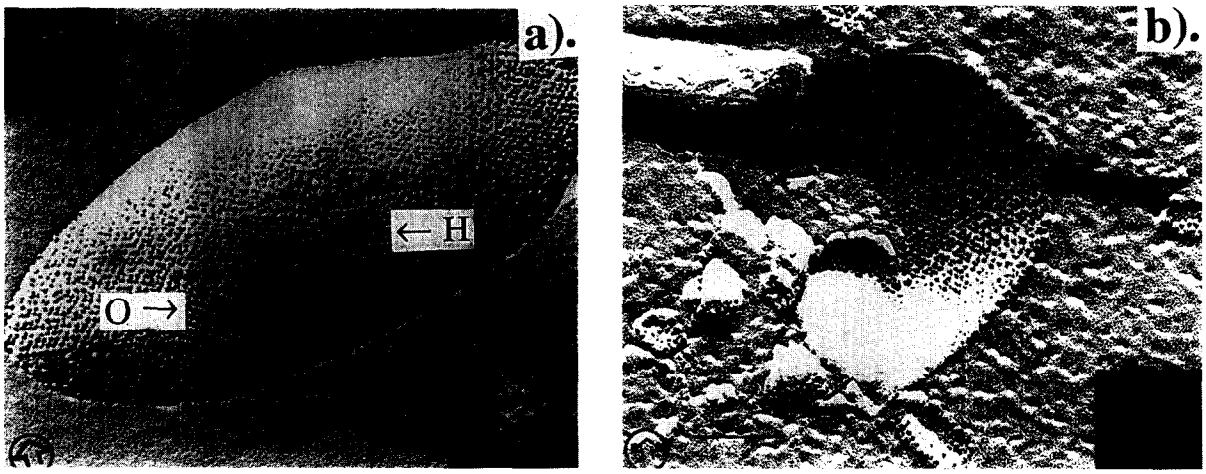

Fig. 7. Freeze-fracture electron micrograph of: (a) purple membrane patch (bacteriorhrodopsin:lipid mole ratio of 1:10 [9]) still containing all the purple membrane lipids into which dimyristoyl phosphatidyl choline (DMPC) had been inserted by a non-specific lipid transfer protein (nsTP) to give a protein:DMPC:PML mole ratio of 1:46:9; (b) delipidated bacteriorhodopsin in a reconstituted complex with dimyristoyl phosphatidyl choline (DMPC) and the diphytanyl phosphatidyl glycerol phosphate (DPhPGP) from *H. salinarium* at a mole ratio of 1:15:5. Both samples were quenched from 55° C in 4 M NaCl. The protein trimers are arranged in an hexagonal array (H) as shown by the optical diffractogram (upper inset of (a); lower inset of (b)) of a selected part of the complex, but in the purple membrane patch derived complex, (a), an orthogonal array (O) is also observed (lower inset). Bar = 100 nm. Shadowing direction shown by arrow. From Refs. [3,4].

6). For these complexes, the protein arrays had similar unit cell dimensions (59 Å) to those measured for bacteriorhodopsin in the purple membrane. Since it has been shown earlier [12] that the protein density alone is insufficient for array formation, it was thought that the lipid in the complexes may play an important rôle in array formation. In addition, is was not clear which lipid of the polar lipid fraction from the purple membrane was important in promoting this behaviour of the bacteriorhodopsin.

3.1.3. Bacteriorhodopsin–dimyristoyl phosphatidylcholine complexes containing purple membrane phospholipids

Complexes that were produced from purple membrane fragments into which dimyristoyl phosphatidyl choline had been inserted using the non-specific transfer protein (Fig. 7a), showed that insertion of the phosphatidyl choline promoted the formation of liposomal structures. The proteins clearly diffuse laterally from the patches into the rest of the liposome since the protein particles are well dispersed throughout the bilayer rather than segregated and still in purple membrane patches.

The insertion of phosphatidylcholine into the purple membrane patches permits the proteins to reform into hexagonal arrays (Fig. 7a; H) as well as permit the formation of an orthogonal array form (Fig. 7a; O), often, as shown here, in the same bilayer. The optical diffractograms confirm this arrangement of protein particles (Fig. 7a), with a unit cell dimension which is about 1/3 larger (at 95 × 59 Å) in the long direction than for the hexagonal packing unit cell.

In an attempt to resolve which one of the lipid species is responsible for the array formation, the individual lipid types from the purple membrane were added separately, together with additional dimyristoyl phosphatidyl choline, in the reconstitution procedure [3]. Thus, phosphatidyl glycerol, the glycolipid, phosphatidyl glycerol phosphate, as well as the sulphated derivative of phosphatidyl glycerol, namely phosphatidyl glycerol sulphate, have been

Fig. 8. Space filling model of a bacteriorhodopsin trimer with cationic residues in positions for potential association with anionic lipids highlighted in blue. Two short chain (for convenience) phosphatidyl glycerol phosphate molecules are shown in yellow in positions of possible interaction with the protein at the polar–apolar interface. (Courtesy of G. Vriend and A. Ulrich, EMBL).

incorporated into the complexes at a range of lipid:protein ratios.

Only bacteriorhodopsin–dimyristoyl phosphatidylcholine complexes which contained phosphatidyl glycerol phosphate or phosphatidyl glycerol sulphate, in the presence of > 2 M NaCl, showed the existence of hexagonal arrays of the protein (Fig. 7b). At all protein densities, protein-free areas were observed, the size of these depending upon the lipid:protein ratio, again implying that the protein density alone is insufficient for array formation. The order in these areas can be very high, giving rise to multiple (up to 3) orders of diffraction in the optical and calculated diffractograms [4].

The unit cell repeat for bacteriorhodopsin in the purple membrane is 59 Å, a dimension which is found in the orthogonal unit cell of 59×99 Å. However, the unit cell for the hexagonal arrays in the various complexes containing dimyristoyl phosphatidylcholine, is between 95 and 99 Å, implying that extra lipid molecules are interspersed inbetween the protein molecules in the reconsituted samples [4].

It is also necessary for > 2 M NaCl to be present with the complex. Dehydrating agents such as tre-

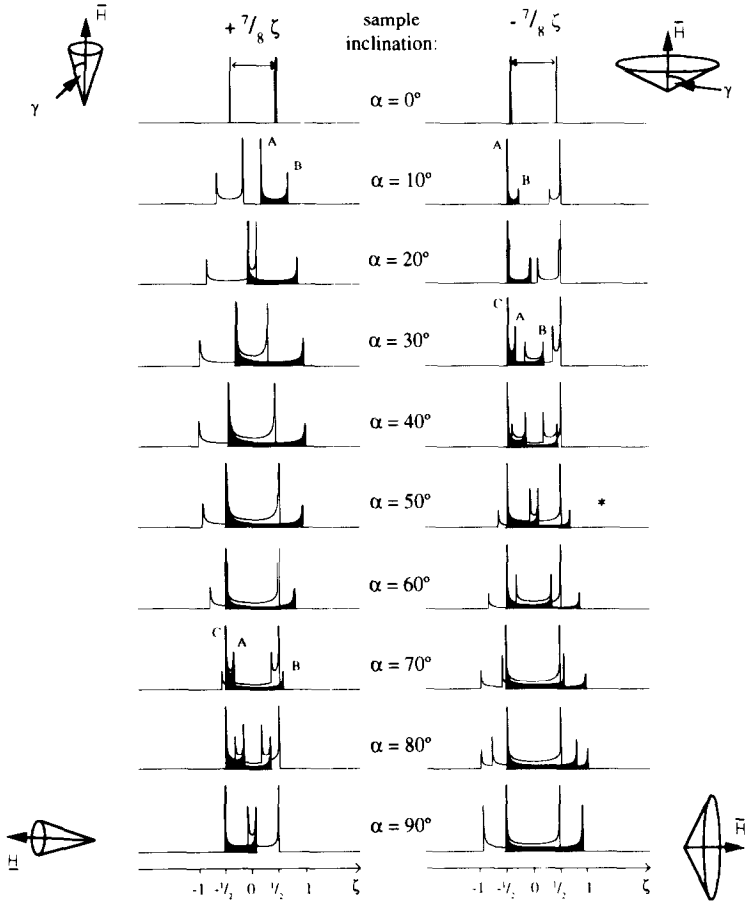

Fig. 9. Two series of theoretical deuterium NMR spectra for a perfectly oriented sample (no line-broadening) tilted at various angles (α) in the applied field. Both simulations have the same quadrupole splitting ($\Delta\nu_Q$), in the zero-tilt spectrum, but of different sign with the positive component of the two nuclear transitions being shaded. The respective bond angles (γ) giving rise to this quadrupole splitting at $\alpha = 0°$ are $\gamma = 38°$ (left column) and $\gamma = 78°$ (right column). The changes in spectral shape at $\alpha \neq 0°$ for each case are clearly distinguished and in particular the spectral width can be seen to be maximum when $\alpha = \gamma$ which permits the sign of $\Delta\nu_Q$ to be determined unequivocably. From Ref. [7].

halose, sucrose and other salts are not able to substitute for NaCl. The effect is thus quite specific.

Molecular modelling (Fig. 8) to try and place phosphatidyl glycerol phosphate head groups near the polar–apolar interface of bacteriorhodopsin has shown that several possible sites exist on the protein for electrostatic associations with the lipid headgroup, should these occur. However, in the profile from 2D electron diffraction, no lipids are identified in specific positions in the purple membrane although this is not too surprising in view of the dynamic characteristics of most lipids in biological membranes thereby leading to a disordered arrangement of any lipids in membranes.

3.2. Determination of methyl group orientations of retinal within bacteriorhodopsin in oriented purple membranes

In principle, the angle of γ between a labelled CD_3-group and the membrane normal can be calculated directly from the quadrupole splitting measured from the deuterium NMR spectrum of the oriented sample aligned with zero tilt ($\alpha = 0$) in the magnetic field. However, since the sign of the splitting cannot be determined, two possible solutions may arise from Eq. (2) and therefore a tilt series of spectra needs to be recorded in order to discriminate the methyl group unequivocably. Computer simulations are used to analyse the deuterium NMR spectra of tilted samples (Fig. 3). The simulated spectra shown in Fig. 9 illustrate the case where two zero-tilt spectra ($\alpha = 0$; top row) have a quadrupolar splitting of the same magnitude but opposite sign (equivalent to ± 35 kHz). For $\alpha \neq 0$ however, the two tilt series in the left ($\gamma = 38°$) and right ($\gamma = 78°$) column exhibit very distinct line-shapes from which the ambiguity of the angle can be immediately resolved by comparison with experimental data. The spectral width is seen to be maximal at $\alpha = \gamma$ (see for example the width of the spectrum in Fig. 9 at $\alpha = 40°$ in the left hand column where $\gamma = 38°$, or in the right hand column at $\alpha = 80°$).

Experimental spectra are broadened through intrinsic and instrumental factors as well as in data manipulation to improve the signal:noise ratio. Fig. 10 illustrates the effects of spectral broadening in the simulations that have to be matched with experimental data. For example, the spectrum for $\alpha = 50°$, $\gamma = 78°$ (marked with an asterisk in Fig. 9) is broadened by a Lorentzian factor to account for the intrinsic line-width (Fig. 10; left column), with no variation in the bond vector. To demonstrate the additional effect of sample mosaic spread, a Gaussian contribution is included in the simulations (Fig. 10; right column) in addition to a typical intrinsic line broadening of 1 kHz (the spectrum chosen for this is marked with an asterisk in the left column of Fig. 10). Typically, a mosaic spread of around 8–10° was required to ensure that experimental and simulated spectra could be matched, and this value was also independently derived from the phosphorus spectra of the same purple membrane samples used in the deuterium NMR. Both the α- and γ-phosphate of the major phosphatidyl glycerol phosphate in the purple membrane are resolved in wide line phosphorus NMR examination of purple membrane patches (Fig. 11), as they were in the high resolution spectra from a detergent solubilized sample [12] (Fig. 4). As

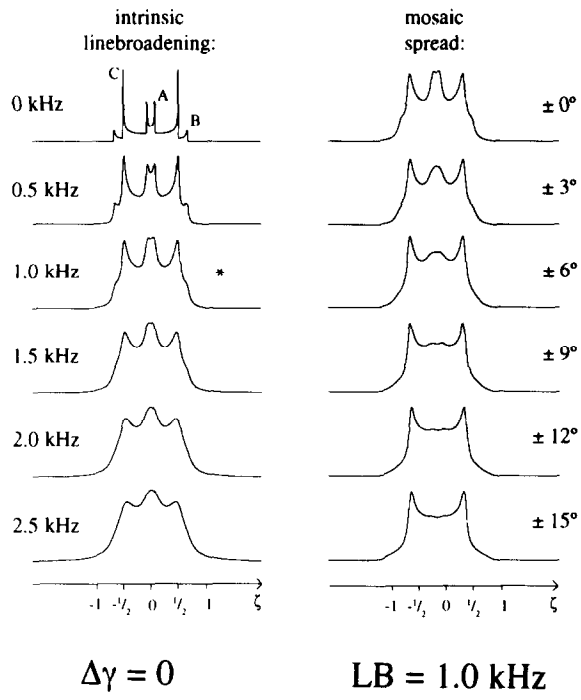

Fig. 10. Calculated deuterium NMR spectral lineshapes for $\alpha = 50°$, $\gamma = 78°$ (example taken from Fig. 9) with increasing intrinsic line-broadening (left column) and spectral broadening due to mosaic spread (right column). From Ref. [5].

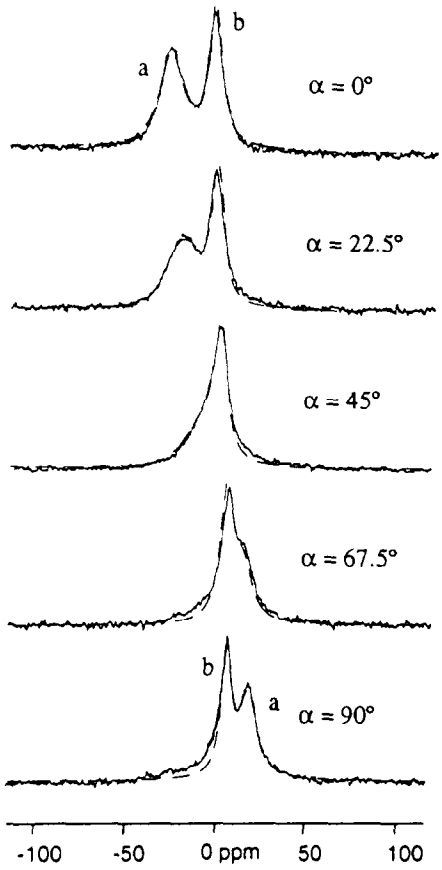

Fig. 11. Experimental phosphorus NMR spectra (solid lines) of a uniaxially oriented sample of purple membrane patches at various inclinations to the applied field. The two phosphate groups of the major phospholipid in the membrane, phosphatidyl glycerol phosphate, are resolved, each having a different chemical shift anisotropy (53 ppm and 13 ppm for the α- and γ-phosphates, respectively). The superimposed spectra in dashed lines were simulated with a line-broadening parameter corresponding to give a mosaic spread (ca. 10°) of the sample which can then be used in the subsequent deuterium NMR spectral analysis. From Ref. [7].

the sample is tilted in the applied field, both resonances sweep through their respective range of the chemical shift anisotropy, which is larger for the more constrained α-phosphate (53 ppm) than for the terminal and more flexible γ-phosphate (13 ppm) and the two lines cross over at the magic angle. These experimental spectra can readily be simulated with a line-broadening that corresponds to a sample mosaic spread typically of 8–10° [7].

The T_1 relaxation time measured for a methyl group on the retinal in bacteriorhodopsin in the purple membrane was approximately 60 ms at −60° C (low temperature improves the signal:noise ratio and leaves the measured quadrupole splitting unchanged when compared to room temperature measurements [7]) confirming that the rotational correlation time is already in the fast motional regime on the deuterium NMR time-scale, with values for τ_c of around 30–40 ps. It is therefore justified to assume fast methyl rotation and omit any contribution to the line-shape from slow motional effects.

Deuterium NMR spectra have been recorded now for all positions of methyls along the retinal in the protein [8]. The experimental spectra and computer simulations for the C_{20} deuterated methyl group of retinal in bacteriorhodopsin are shown in Fig. 12. The angular variation of the sample gives rise to well defined spectral changes which can be simulated with a quadrupole splitting from the zero-tilt spectrum of 46 kHz and a bond angle of 32° for the $-CD_3$ group with respect to the membrane normal [6]. The spectra in Fig. 12 have a value of $\Delta\nu_Q > \Delta\nu_Q^{(powder)} = 40$ kHz, and thus there is no ambiguity in the sign of the quadrupole splitting needed to calculate the bond angle. However, for the C_{19} position, $\Delta\nu_Q = 30$ kHz which could have either a positive or negative sign, thereby yielding very different possible solutions to Eq. 2 (see Fig. 9). Thus, only through a tilt series of experimental spectra (Fig. 12; central column) and comparison with simulations (right and left columns) can the sign be resolved. A value of $\Delta\nu_Q = +30$ kHz (Fig. 12; left column) produces the spectra which correspond with the experimental spectra in Fig. 13 and thus gives a bond angle of $\gamma = 40°$ while other solutions of $\gamma = 73°$ (right-hand column) can be excluded [8].

In all cases, the spectra could be simulated uniquely at each angle of tilt of the purple membrane patch with respect to the applied field. Due to the sensitivity of the method (changes in quadrupole splitting of 2–3 kHz out of a full range of 40 kHz produce large changes in the spectra), and the fact that each spectrum is a unique piece of experimental information, the methyl group orientations are well resolved to a high (±2°) level of precision [6]. However, one aspect which is not addressed is the absolute sidedness of the protein, since this is not

resolved in the method and the spectra do not discriminate angles above or below the horizontal. Nevertheless, from the known connectivities of a set of methyl groups, their relative orientations with respect to one another can be inferred.

The measured values for the bond angles are given in Fig. 14. The 6-*S*-trans conformation of the cyclohexene ring is immediately evident from these results. The molecular plane must sit approximately upright in the protein in view of the roughly horizontal geminal methyl groups (C_{16} and C_{17}) on the ring (Fig. 2). Since the vectors for the C_{18}, C_{19} and C_{20} positions are not entirely parallel, this indicates an in-plane curvature of the conjugated chromphore long axis and possibly an out-of-plane twist (Fig. 15). Optical anisotropy experiments [14] and neutron diffraction [5] have given indications of this possibility but the results from those investigations can only provide information about an average chromophore orientation within the protein. Studies are currently underway to resolve whether the chromophore changes its orientation in the protein during the

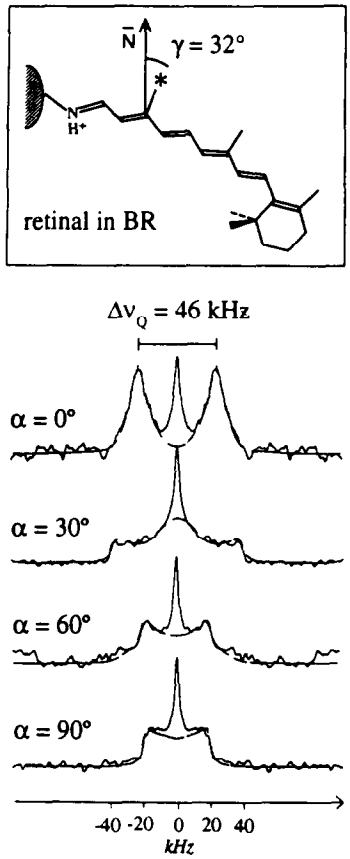

Fig. 12. Experimental (solid lines) and simulated (dashed lines) deuterium NMR spectra at room temperature for C_{20} deuterated retinal in bacteriorhodopsin in purple membrane patches at various tilt angles with respect to the applied field. The quadrupole splitting at $\alpha = 0°$ is 46 ± 1 kHz which gives a bond angle of $\gamma = 32 \pm 1°$ with respect to the membrane normal. The central spectral component is due to residual HDO in the sample. From Ref. [5].

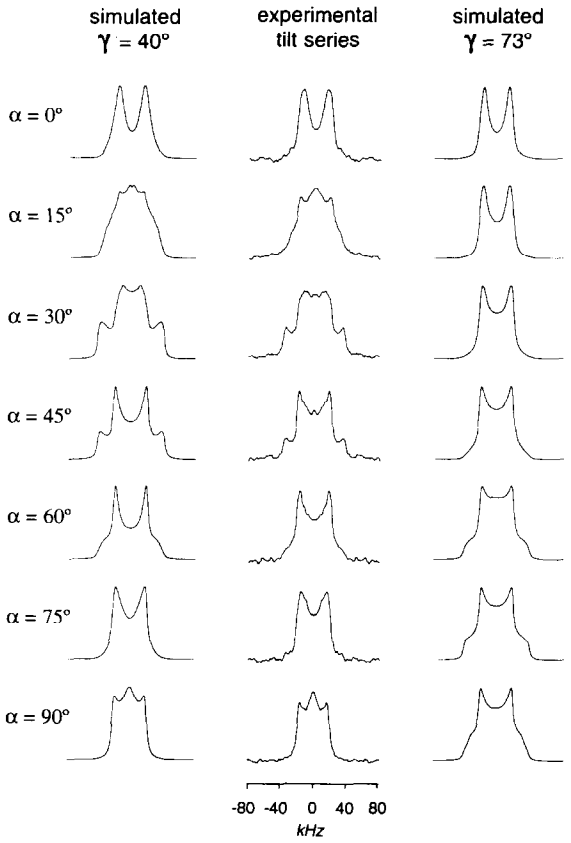

Fig. 13. Experimental series of deuterium NMR spectra for the central methyl group (C_{19}) labelled on retinal in bacteriorhodopsin in an oriented purple membrane sample at $-60°$ C (middle column). The experimental series at various tilt angles (α) of the sample with respect to the applied field is compared with the simulated spectra for identical values of the quadrupole splitting, $\Delta\nu_Q$, of 30 kHz at $\alpha = 0°$ but with a positive (left column) and negative (right column) sign for $\Delta\nu_Q$. The simulated spectral line-shape clearly show that only with a positive sign of $\Delta\nu_Q$ (left column) are the experimental and computed line shapes equivalent. The value of γ is therefore 40° and not 78°. From Ref. [8].

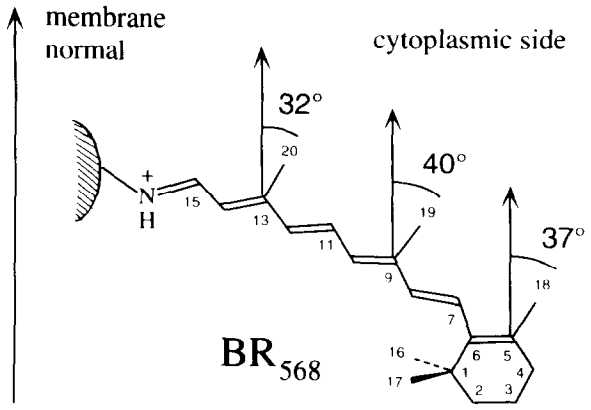

Fig. 14. Structure of retinal showing the orientation and conformation of the molecule when in the binding site within the protein in purple membrane patches as deduced, ab initio, from the bond angles measured in the deuterium NMR experiments. Angles are within $\pm 2^{\circ}$. From Ref. [8].

photocycle, especially when trapped in the M-state (Ulrich et al., in preparation).

4. Discussion

4.1. Array formation of bacteriorhodopsin

Bacteriorhodopsin has been reconstituted into dimyristoyl phosphatidylcholine bilayers previously [10]. In these reports, the protein was still seen to arrange itself into hexagonal arrays in the membrane. The protein had been isolated using LDAO or cholate as detergents and no special precautions were taken to remove endogenous purple membrane lipids. In our studies [3,4,12] we have been careful to remove endogenous purple membrane phospholipids and reconstitute bacteriorhodopsin into dimyristoyl phosphatidylcholine as the only bilayer lipid. In the absence of endogenous purple membrane lipids, no array formation is observed. When endogenous lipids are present, either in purple membrane patches into which phosphatidyl choline has been inserted or in phosphatidyl choline complexes with controlled added amounts of phosphatidyl choline phosphate or the sulphate derivative, then arrays do reform. The orthogonal array observed in the former type of complex (Fig. 7a) has been described previously in purple membranes which had been partially delipidated by detergent [15], again implying the importance of the role of lipids in protein array formation. Also, this observation would imply that it is not the orientation (which way up) of the protein in the complex which determines the form of the array, but possibly hydrophobic protein-bilayer matching.

The major phospholipids in the purple membrane (Fig. 1) have highly branched alkyl chains and a charged (3 −ve charges) head-group and the array formation of bacteriorhodopsin is only possible with one of these phospholipid types, namely either phosphatidyl glycerol phosphate or the sulphate derivative. One other integral membrane protein, the light

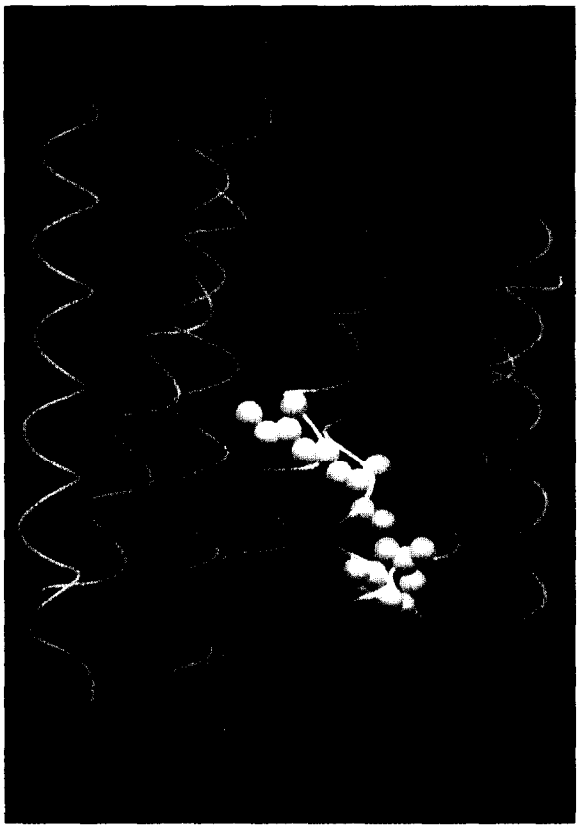

Fig. 15. Retinal (purple) is embedded in the centre of the seven transmembrane helices (in yellow) of bacteriorhodopsin at the chromophore binding site. The NMR and molecular modelling studies show that the polyene chain is curved towards the extracellular side of the membrane and the cyclohexene ring is 6-S-trans with respect to the chain.

harvesting complex (LHC II) from chloroplasts, has also shown similar behaviour, having a requirement for glycolipid indigenous to the natural membrane [16]. Such specific protein:lipid interactions may be due to head group or acyl (or alkyl) chain interactions, but this has not yet been fully resolved. Indeed, the rather rigid diphytanyl chains of the purple membrane lipids could act to minimise the free energy of interaction between trimers, thus enabling the entropic contribution to protein disordering to be overcome. Alternatively, a simple electrostatic interaction between trimers mediated through the head groups of charged lipids, could have the same effect. What is not clear is the involvement of NaCl in the mechanism of array formation, since no arrays are formed in the absence of > 2 M NaCl, with sucrose, trehalose or polyethylene glycol unable to substitute for NaCl. The Na^+ may induce conformational changes in the protein which are required for protein–lipid or protein–protein interactions to occur. Formation of 3D crystals of bacteriorhodopsin is also affected by the presence of lipids [17], and thus lipid contamination or the control of lipid content in such crystallisation trials may be rather important and may have been overlooked in the past.

The clear implication of such observations is that in all attempts to produce 2D arrays or 3D crystals of integral membrane proteins, the composition of the crystallisation milieu needs to be carefully controlled. Although the lipid composition does introduce another variable into the process, it may be an essential variable and little is known currently about how to make membrane protein crystals in any kind of routine way, so that such factors should be monitored and recorded.

4.2. Retinal structure in bacteriorhodopsin

Membrane protein structure determinations to atomic resolution are not routine for many reasons, not least those discussed above (Section 4.1). Thus, alternative methods are essential if the structure and function relationships of this class of protein, which includes receptors and transport proteins, are to be resolved. Solid state NMR methods are now becoming sufficiently well advanced so that orientation, conformation and inter-atomic distances of selectively isotopically labelled groups can be resolved within integral membrane proteins. Problems with the production of sufficient amounts of protein either of a wild type or an expressed derivative, as well as isotopic labelling of the parts of the protein of interest, are being resolved. Finally, the analysis of NMR spectra and molecular modelling methods are being developed to keep pace with the biochemical advances, such that the use of solid state NMR to resolve membrane protein structure will become feasible for more examples.

The orientation of the retinal chromophore in bacteriorhodopsin is sufficiently well resolved in these present studies [6–8] to provide an independent, ab initio description of the overall chromophore alignment and its intramolecular conformation, in good agreement with known pieces of information from other biophysical techniques [5,14]. It is found here that the tilt and curvature of the retinal are somewhat steeper than the average orientation of the chromophore long axis detected by optical anisotropy measurements [14] and neutron scattering [5]. This may be due to a deviation of the transition moment from the long axis of the conjugated system of double bonds [18] and due to the local details detected in the present work. Also, the steric effects of the chain methyls are observed in the current study as a distinct distortion, since the orientations of each individual methyl group could be measured directly.

All the NMR experiments described here were performed in the dark adapted, ground state of the protein where there exists a 1:2 mixture of the all-*trans* and the 13-*cis*,15-*syn* retinal isomers. Since only a single spectral component was resolved for each of the methyl groups along the polyene chain [8], it is concluded that the thermal isomerization of the Schiff base end of the retinal around the $C_{13}{=}C_{14}$ double bond and simultaneously the $C_{15}{=}N$ bond, has no effect on the orientation of the remainder of the chain on which the methyl groups reside [7,8] thus confirming a measurement of the transition moments of the light and dark adapted states of the bacteriorhodopsin which are found to differ by $< 0.4°$ [14]. The deuterium NMR method is particularly sensitive to orientational changes in this spectral range, and thus it should be able to detect whether the retinal undergoes any changes in orientation at the local deuteromethyl probes during the photocycle (work in preparation).

Acknowledgements

Valuable comments from A. Ulrich, B. Sternberg and C. Whiteway are gratefully acknowledged. The colour figures were generously produced and supplied by Gert Vriend, EMBL, Heidelberg, Germany. This work was supported financially by the EU, MRC, SERC and DFG.

References

[1] H. Michel, Crystallization of Membrane Proteins, CRC Press, 1989.
[2] R. Henderson, J.M. Baldwin, T.A. Ceska, F. Zemlin, E. Beckman and K.H. Downing, J. Mol. Biol., 213 (1990) 899.
[3] B. Sternberg, C. L'Hostis, C.A. Whiteway and A. Watts, Biochim. Biophys. Acta, 1108 (1992) 21.
[4] B. Sternberg, A. Watts and Z. Cejka, J. Struct. Biol., 110 (1993) 196.
[5] T. Hauß, Dissertation, Verlag für Wissenschaft und Bildung, Berlin, 1993.
[6] A.S. Ulrich and A. Watts, Solid State NMR, 2 (1993) 21.
[7] A.S. Ulrich, M.P. Heyn and A. Watts, Biochemistry, 31 (1992) 10390.
[8] A.S. Ulrich, A. Watts, I. Wallat and M.P. Heyn, Biochemistry, 33 (1994) 5370.
[9] D. Oesterhelt and W. Stoeckenius, Methods Enzymol., 31 (1974) 667.
[10] R.J. Cherry, U. Müller, R. Henderson and M.P. Heyn, J. Mol. Biol., 121 (1978) 283.
[11] K.S. Huang, H. Bayley and H.G. Khorana, Proc. Natl. Acad. Sci. USA, 77 (1980) 323.
[12] B. Sternberg, P. Gale and A. Watts, Biochem. Biophys. Acta, 980 (1989) 117.
[13] J. Seelig, Q. Rev. Biophys., 10 (1977) 353.
[14] G.F.X. Schertler, R. Lozier, H. Michel and D. Oesterhelt, EMBO J., 10 (1991) 2353.
[15] H. Michel, D. Oesterhelt and R. Henderson, Proc. Natl. Acad. Sci. USA, 77 (1980) 338.
[16] W. Kühlbrandt, Q. Rev. Biophys., 25 (1992) 1.
[17] A. Watts, C. Venien-Bryan, M. Sami, C. Whiteway, J. Boulter and B. Sternberg, in A. Watts (Editor), Protein–Lipid Interactions, Elsevier, Amsterdam, 1993, p. 351.
[18] Q.-y. Shang, X. Dou, and B.S. Hudson, Nature, 352 (1991) 703.